Atmos. Chem. Phys. Discuss., 11, 3461–3492, 2011
www.atmos-chem-phys-discuss.net/11/3461/2011/
doi:10.5194/acpd-11-3461-2011
© Author(s) 2011. CC Attribution 3.0 License.

Atmospheric Chemistry and Physics Discussions

This discussion paper is/has been under review for the journal Atmospheric Chemistry and Physics (ACP). Please refer to the corresponding final paper in ACP if available.

Condensational uptake of semivolatile organic compounds in gasoline engine exhaust onto pre-existing inorganic particles

S.-M. Li[1], J. Liggio[1], L. Graham[2,*], G. Lu[1], J. Brook[1], C. Stroud[1], J. Zhang[1], P. Makar[1], and M. D. Moran[1]

[1]Air Quality Research Division, Atmospheric Science and Technology Directorate, Science and Technology Branch, Environment Canada, 4905 Dufferin Street, Toronto, Ontario M3H 5T4, Canada
[2]Air Quality Research Division, Atmospheric Science and Technology Directorate, Science and Technology Branch, Environment Canada, 335 River Road, Ottawa, Ontario K1A 0H3, Canada
[*]now at: Department of Chemistry, University of Christchurch, Canterbury, 8041, New Zealand

Received: 29 November 2010 – Accepted: 17 January 2011 – Published: 31 January 2011

Correspondence to: S.-M. Li (shao-meng.li@ec.gc.ca)

Published by Copernicus Publications on behalf of the European Geosciences Union.

Abstract

This paper presents the results of laboratory studies on the condensational uptake of gaseous organic compounds in the exhaust of a light-duty gasoline engine onto pre-existing sulfate and nitrate seed particles. Significant condensation of the gaseous organic compounds in the exhaust occurs onto pre-existing inorganic particles on a time scale of 2–5 min. The amount of condensed organic mass (COM) is proportional to the seed particle mass, suggesting that the uptake is due to dissolution, not adsorption. The solubility decreases as a power function with increased dilution of the exhaust, ranging from 0.23 g/g at a dilution ratio of 81, to 0.025 g/g at a dilution ratio of 2230. The solubility increases nonlinearly with increasing concentration of the total hydrocarbons in the gas phase (THC), rising from 0.12 g/g to 0.26 g/g for a C_{THC} increase of 1 to 18 $\mu g\,m^{-3}$, suggesting that more organics are partitioned into the particles at higher gas phase concentrations. In terms of gas-particle partitioning, the condensational uptake of THC gases in gasoline engine exhaust can account for up to 30% of the total gas+particle THC. By incorporating the present findings, regional air quality modelling results suggest that the condensational uptake of THC onto sulfate particles alone can be comparable to the primary particle mass under moderately polluted ambient conditions. These findings are important for modelling and regulating the air quality impacts of gasoline vehicular emissions.

1 Introduction

Airborne particles are known to pose serious health risks (Dockery et al., 1993; Geller et al., 2006; Schwarze et al., 2006; Pope III and Dockery, 2007; Brook et al., 2010) and have a large influence on the Earth's climate (Jacob and Winner, 2009). Such impacts are increasing public and government scrutiny of particulate matter (PM) emissions from all anthropogenic activities. Primary PM from automotive engine exhaust is among the most studied and regulated emissions over recent decades; yet to

ACPD
11, 3461–3492, 2011

conform with current regulations, automotive emissions of primary particles are determined on a mass basis which ignore complex at-source processes that re-distribute the semivolatile organic compounds (SVOCs) between gas and particle phases. Standard automotive PM mass emission measurements, based on sampling on filters and gravimetric analysis, have proven to be artifact-prone, particularly at low emissions levels (Chase et al., 2004; Lipsky and Robinson, 2006). Determining PM levels in emissions at dilution levels spanning several orders of magnitude can be a significant challenge, affected by even the slightest details in the vehicle testing and sampling protocols. Direct particle size distribution measurements are now a recommended method to characterize particle emission from engine exhaust, particularly with the recent focus on the particle number concentrations in newer standards, such as EURO 5 and 6 (European Commission, 2008).

The most difficult measurement challenge arises from the highly dynamic situations of cooling and dilution upon mixing with the ambient atmosphere, where the steady-state equilibrium between gases and particles in the exhaust is easily shifted. This can lead to changes in the physical and chemical characteristics of particles. Notable recent studies have focused on the impacts of ambient temperature and dilution on PM emissions (Lipsky and Robinson, 2006; Grieshop et al., 2009) and low ambient temperature is known to result in the enhanced formation of nucleation mode particles in gasoline and diesel vehicle exhaust (Mathis et al., 2004, 2005). Robinson et al. (2007) demonstrated that upon dilution, diesel exhaust PM decreases due to evaporative loss of SVOCs from the particles. Gasoline engine particulate emissions are less well studied; but a similar dilution effect on primary particles in gasoline engine exhaust can be expected.

What has not been considered in the automotive primary PM emission studies to date is the condensational uptake/evaporation of gaseous pollutants to and from pre-existing ambient particles upon the initial mixing of engine exhaust with ambient air. Theories of gas-particle partitioning dictate that at least some of the SVOCs in exhaust gases will condense and reach equilibrium with ambient particles under atmospheric

ACPD
11, 3461–3492, 2011

conditions. There is circumstantial evidence pointing to this re-partitioning within exhaust gases (Kittelson, 1998; Khalek et al., 1999; Maricq et al., 1999; Mathis et al., 2004; Lipsky and Robinson, 2006). For example, diesel primary particles are known to contain solid cores of soot with adsorbed hydrocarbons, nitrates and sulfates (Sakurai et al., 2003; Kwon et al., 2003), and there is evidence that the growth of the nucleation mode particles is partially attributable to condensation (Mathis et al., 2004). The adsorbed hydrocarbons are in dynamic equilibrium with the gas phase, moving in and out of the primary particles as temperature and concentration change. Such processes should also occur once the gaseous exhaust comes into contact with ambient particles that provide surfaces or volumes for uptake to occur, but few studies have reported on the uptake process onto ambient particles, and it is not known how significant this process is in terms of release of primary PM into the ambient atmosphere. Although this uptake takes place in the atmosphere after exhaust, the time and spatial scales associated with mixing and dilution at tailpipe and uptake of gases on ambient particles are from seconds to minutes and from tens to hundreds of meters. Hence from the standpoint of health impacts and from atmospheric models, the condensed SVOC species will be hard to distinguish from primary PM mass.

The present study addresses the condensational uptake of organic gaseous pollutants on ambient particles. PM emissions studies focused on gasoline engine exhaust are relatively few compared to those on diesel exhaust, since exhaust PM levels of modern catalyst-equipped, properly-operating gasoline engines are low. In this study, the magnitude of the condensational uptake of organic materials in gasoline engine emissions is quantified, and a parameterization of the condensational uptake onto pre-existing particles is derived, and this parameterization is used in a regional air quality model to assess the impact of this process on a regional basis.

ACPD
11, 3461–3492, 2011

2 Experimental design

The experiments were carried out using the setup illustrated in Fig. 1. This setup consisted of two sections, an engine testing facility from which the primary PM measurements were made, and a flow tube where the gas uptake and condensation on pre-existing particles was investigated.

2.1 Gas and primary particle emissions measurements

In the engine testing facility, a multi-port injected gasoline engine, recovered from a 1991 model year General Motors Lumina light duty vehicle, was equipped with a new but degreened original equipment three-way catalyst. The engine was installed on a dynamometer and enclosed in a controlled-access test room. The engine exhaust was directly vented into a constant volume sampling (CVS) system, where it underwent primary dilution with a dilution ratio between 14–22 (Table 1), and was kept at an ambient temperature of 25 °C.

Concentrations of CO, CO_2, NO_x and total hydrocarbon (THC) in the primary dilute exhaust in the CVS were monitored using non-dispersive infrared analyzers for CO and CO_2, chemiluminescence analyzers for NO_x ($NO + NO_2$), and a flame ionization detector for THC. The analyzers were zeroed and spanned to adjust for instrument drift every 30 min. The flame ionization detector was calibrated with propane and reported concentration of THC in ppmC.

Primary particles in the CVS were characterized with a scanning mobility particle spectrometer (SMPS, TSI model 3080) using a differential mobility analyzer (nano-DMA) column (TSI model 3085) and a TSI model 3025A condensation particle counter (CPC) for sizing particles from 4.6 to 162.5 nm diameter. The SMPS scanned over the size range on a 3-min scanning cycle. A second CPC (TSI model 3022A) was used to monitor the particle number concentrations, for particles as small as 7 nm. The second CPC monitored secondary dilute exhaust after second-stage dilution using Dekati ejection diluters, either one or two in series. The single diluter achieved a 7:1

ACPD
11, 3461–3492, 2011

dilution from the primary dilute exhaust in the CVS, and two in series achieved a 56:1 dilution.

2.2 Engine operation mode

During the experiments, the engine was operated in three modes of engine speed (shown by the rotation per minute, RPM) and load that simulate different driving conditions (Table 1). The engine was run continuously for several hours in each mode that was necessary for the condensational uptake experiments. For the experiments, the engine was operated on Canadian commercial summer grade gasoline with sulphur content <30 ppm. The CVS system was operated at a fixed total volume flow rate (F_{CVS}) of 21.24 m^3/min. Thus, depending on the RPM, the primary dilution ratio, defined as $F_{CVS}/F_{exhaust}$, varied over a range of 14.1 to 22.3 (Table 1). Concentrations of CO, CO_2, NO_x and THC in the primary dilute exhaust in the CVS were monitored every second in repeated 30-minute segments.

2.3 Condensational uptake experimental setup

The flow tube setup, depicted in Section B of Fig. 1, is designed to measure the condensational uptake of gases on particles. In these studies, laboratory-generated seed particles were used as surrogates for ambient inorganic particles. The flow tubes were Teflon-coated stainless steel tubes of 2.54 cm inner diameter and 30 cm length. A total of 13 tubes were connected together using connectors equipped with sampling ports. Three air streams were delivered into the flow tubes (streams a, b, and c, Fig. 1), one carrying the primary gas exhaust (stream a), one carrying zero air for dilution (stream b), and one carrying seed particles (stream c). At the end of the flow tubes, a probe was used to measure the relative humidity (RH) and temperature of the mixture in the flow tubes.

Seed particles were generated by atomizing a solution of $H_2SO_4/(NH_4)_2SO_4$ with a constant volume atomizer (TSI model 3076) with compressed zero air generated

ACPD
11, 3461–3492, 2011

from a zero air source (AADCO model 737). Depending on the experiment, the ratio of H_2SO_4 to $(NH_4)_2SO_4$ in the solution was chosen to give different initial particle acidities; however, in most experiments the sampled particles were neutral after exposure to NH_3 in the engine exhaust in the flow tube. In a few experiments, NH_4NO_3 particles were generated instead of sulfate particles. These particles were dried using a diffusion dryer (TSI model 3062), and size selected using a TSI SMPS/DMA model 3080/3081 before being delivered into the flow tubes.

The seed particles were introduced into the first flow tube at its central axis through 1/4 inch outer diameter (o.d.) stainless steel tubing. This was designed with a coaxial introduction of the primary dilute exhaust gas. The dilute exhaust was pumped from the CVS using a Teflon diaphragm pump through a HEPA filter to remove the primary particles (stream a). This particle-free exhaust gas was introduced into the first flow tube through a 1/8 inch o.d. stainless steel tube that is nested at the centre of the 1/4 inch line used to introduce the particles. Entry linear velocities of both the seed particle flow and the exhaust gas flow into the flow tube were maintained to be the same in some experiments, although it was found that the effect of initial linear velocities of either the particles or the exhaust gases was minimal. Thus, both the particles and the dilute exhaust gas traveled down the flow tubes concentrically along the axis of the flow tubes. The mixing of the exhaust gas and the seed particle flows from their introduction at the first flow tube constituted a secondary dilution, with a dilution ratio determined by the flow rates from both flow streams a and c in Fig. 1. In a few experiments, extra dilution was made with an additional flow stream of zero air (flow stream b in Fig. 1).

Sampling of particles was made at the central axial position in the air stream flowing down the flow tubes through a 1/4 inch stainless steel tube inserted radially through selected sampling ports. Depending on the experiment, a tertiary dilution was made at the 1/4 inch sampling port that also helped balance the flows. After the tertiary dilution, the 1/4 inch stainless steel sampling line was split and fed to three instruments, an aerosol mass spectrometer (AMS), a CPC (TSI model 3775), and a proton transfer reaction mass spectrometer (PTRMS). The contact time between the seed particles

ACPD
11, 3461–3492, 2011

and the diluted exhaust varied from 1.5 to 7 minutes, depending on the total flow rate through the flow tubes and the position of the sampling port, as further discussed below. Residence time in the sampling line was approximately 1 s.

The particle chemical composition and mass were monitored using an Aerodyne Research Inc high resolution time-of-flight aerosol mass spectrometer (HR-ToF-AMS; DeCarlo et al., 2006). The HR-ToF-AMS was operated in the high sensitivity mode (V-mode) with a 2-minute time resolution. Particle sulfate, nitrate and ammonium size distributions were monitored using the particle time-of-flight mode of the HR-ToF-AMS.

2.4 Uptake and condensation conditions

Experimental conditions were designed to target each of five controlling factors on the uptake and condensation, including relative humidity, duration of exposure, chemical composition, sizes of seed particles, and dilution ratios. Table 2 shows the range of the factors that were varied to determine the impacts of these factors. During all experiments, temperature in the air flow inside the flow tube varied in a narrow range of 23.5–28.8 °C, whereas the RH changed from 6.5% to 33.5%, resulting from the mixing of high RH in the engine exhaust with the dilution air.

The HR-ToF-AMS measures particle chemical composition between 50 – 700 nm vacuum aerodynamic diameter (Liu et al., 2007); in the present experiments, the monodispersed seed particles were selected from 150 to 450 nm mobility diameter (d_m), equivalent to 206 to 619 nm vacuum aerodynamic diameter (d_{va}) for NH_4NO_3 particles. Secondary dilution ratios at the introduction point of the seed particles/primary exhaust gases into the flow tubes varied between 11 to 200, resulting in a total dilution ratio range of 81 to 2230. No active control of RH and temperature was used, and thus the RH was mostly influenced by the water vapor in the primary gas exhaust mixing with zero air, resulting in a relatively low RH of 33% in the flow tubes. Even in this low range, the seed sulfate particles are expected to be deliquescent (Onasch et al., 1999) and the nitrate particles are expected to contain water with the organic contents (Prenni et al., 2003).

ACPD
11, 3461–3492, 2011

3 Results and discussions

3.1 Characterization of primary dilute gaseous emissions

The average THC and NO_x concentrations in the primary dilute exhaust in the CVS for the multiple repeats of each engine mode are listed in Table 1. CO was below the instrument detection limit in the primary dilute exhaust except during idling, indicating that the catalyst reached its minimum operating temperature for all three modes. The NO_x concentration for Mode 1 was about 3 times higher than for Modes 2 and 3, reflecting the higher torque of this mode that requires significantly higher fuel burns and higher combustion temperature than the other two modes. As a result, THC concentrations, expressed in ppmC, was also typically higher for Mode 1 than the other modes, even though it varied within a narrow range of 5.5–6.8 ppmC among the three modes, reflecting the relatively stable working conditions of the catalyst. On the other hand, the ratio THC/CO_2, a surrogate for the emission factor for THC, was the lowest for Mode 1 at $(6.5\pm0.2)\times10^{-4}$ compared with those for Mode 2 and 3 at $(1.0\pm0.1)\times10^{-3}$, and $(7.1\pm0.4)\times10^{-4}$, respectively, indicating a more efficient fuel combustion at higher temperature. The SVOCs in the THC mixture, not separately quantified, are expected to be in equilibrium with organics in the primary particles in the exhaust. The SVOCs are also available for further condensation onto existing ambient particles once the exhaust gas is mixed with the ambient air. This process and the resulting particle mass is not measured in motor vehicle emissions testing since the exhaust is diluted and mixed with particle free (HEPA-filtered) air in standard testing methods.

3.2 Condensational uptake of SVOCs onto existing particles

Condensation of SVOCs in engine exhaust onto existing ambient particles is expected to occur once the SVOCs come into contact with these particles. This re-partitioning of organic mass from gas to particle represents a reverse to the process of primary particle evaporation upon dilution (Robinson et al., 2007) and results in, we hypothesize, a

ACPD
11, 3461–3492, 2011

non-negligible source of low bias in the current vehicular particle mass emission data.

To determine the magnitude of condensation, laboratory generated seed particles of inorganic composition were used as surrogates for inorganic particles in ambient air. The seed particles were exposed to the gaseous exhaust under different experimental conditions as shown in Table 2.

Condensational uptake of SVOCs onto the particles was observed in all experiments. To generalize the main findings, this organic uptake has approximately a linear dependency on the available seed particle mass as represented by sulfate under each set of experimental conditions. Experiments using different chemical compositions (nitrate vs. sulfate) for the seed particles revealed similar linear relationships. Different exposure times of the particles to the THC, between 1.5 to 7 minutes, produced no discernable differences in the condensational uptake. On the other hand, the exposures to different levels of THC resulted in linear dependencies with significantly different slopes. These THC levels varied over orders of magnitude due to a combination of different engine running modes (Table 1) and different dilution ratios.

To illustrate these general findings, Fig. 2a shows the results obtained for Mode 2 experiments on 25 April, revealing the condensed organic mass (COM) as an approximately linear function of seed particle sulfate mass. In these experiments, the seed particles were neutral, and the total dilution ratio of the gaseous exhaust was kept constant at 395 resulting in a constant THC (Tables 1 and 2). Furthermore, the contact time between the seed particles and the diluted gaseous exhaust remained constant at 5.5 min. The variables in the experiments shown in Fig. 2a are the particle sizes and number concentrations of the seed particles that resulted in different seed particle mass loadings. The linear dependency of the COM on the seed particle sulfate is highly significant ($r^2 = 0.95$).

3.3 Dilution effects on the condensation processes

Once engine exhaust comes in contact with pre-existing particles, re-partitioning of SVOCs between the particles and the gas phase is expected, resulting in SVOC

ACPD
11, 3461–3492, 2011

condensation onto the pre-existing particles until a steady state is reached. As demonstrated above, organic materials are taken up onto the seed particles as a result of the re-partitioning. A steady-state of COM with gas phase concentrations is expected to be established in milliseconds to seconds for the typical accumulation mode ambient aerosol particles (Seinfeld and Pandis, 1998), and COM is expected to be influenced by the vapor pressures of the SVOCs, and hence by the degree of dilution. Figure 2a shows that under one dilution ratio, COM depends linearly on the seed particle mass regardless of the particle sizes (from 150 to 450 nm), i.e.,

$$\mathrm{COM} = a + S \cdot M_s \tag{1}$$

where M_s is the mass concentration of the seed particles in a unit air volume and dominated by $SO_4^=$, and COM is the amount of condensed organic mass concentration in the same air volume, again determined by the HR-ToF-AMS. Results show that under most experimental conditions, the intercept a is not significantly different from 0. Therefore, the slope of the curve S can be given by,

$$S = \frac{\Delta \mathrm{COM}}{\Delta M_s} = \mathrm{COM}/M_s \tag{2}$$

The uptake was a result of either adsorption onto the surface of the seed particles, or dissolution into the seed particles, or a combination of the two. To determine which process was responsible, S is derived following Eq. (2) for each of the five sizes of the seed particles for the experiments shown in Fig. 2a, and plotted in Fig. 2b as a function of the surface area of a single seed particle for the five sizes. Also plotted in the Figure 2b are ratios of COM/M_s for either the pure dissolution (blue dash line) and adsorption processes (red dash line) versus the surface area of a single particle. For dissolution process that reaches equilibrium with gas phase, the ratio COM/M_s is the solubility and remains a constant for different single particle sizes. Adsorption of organics onto the seed particles, on the other hand, depends on the available surface area, leading to an inverse relationship between the ratio COM/M_s and particle surface area. Figure 2b clearly shows that COM is due to dissolution rather than surface adsorption, having

ACPD
11, 3461–3492, 2011

exhibited no dependence on the particle surface area. Since COM comprises individual compounds, S can be better described as an aggregate solubility of the SVOCs in the seed particles, from the sum of the masses of individually dissolved SVOC species.

Figure 3 shows the results of experiments specifically designed to test the response of S to different final dilution ratios over a range from 81 to 2230. Plotted in the figure is S versus the dilution ratios. Both seed particles of either $(NH_4)_2SO_4$ or NH_4NO_3 composition were used in the experiments. The results in Fig. 3 are for near constant RH and temperature, but for different seed particle composition and sizes.

There is a marked decrease in S as the dilution ratio (D) increases. Such a dependency is similar to those reported for the primary particle mass emissions in low-load diesel engine exhaust and in wood smoke exhaust (Lipsky et al., 2006). Robinson et al. (2007) showed a declining primary organic mass emission factor of diesel engines as a function of dilution ratio. For the gasoline exhaust studied here, a power function

$$S = (0.025 \pm 0.09) + 7305\ D^{-(2.39\pm0.03)} \quad (3)$$

was fitted to the data, D being the dilution ratio, with a correlation coefficient $r^2 = 0.90$ for the fit. The value of S dropped from 0.23 g/g at D =81, to 0.025 g/g at $D = 2230$, dropping by a factor of 9.2. In comparison, for diesel exhaust particles, a reduction by a factor of approximately 2 is reported over the same dilution range but this was attributed to the volatility of SVOCs on the diesel particles (Robinson et al., 2007).

3.4 Comparison of primary particles with COM

The primary particles coming out of the gasoline engine were likely dominated by organics, and the partitioning between the gas phase and the primary particles should be described by the saturation vapor pressures of compounds in the THC mixture in the exhaust. Unfortunately, no primary particle mass and THC data were collected in the flow tubes for the direct comparison. However, this partitioning between the gas phase and the primary particles in the exhaust in the CVS can be calculated. First, the primary organic aerosol (POA) mass concentration, C_{pp}, is estimated using

ACPD
11, 3461–3492, 2011

the particle size spectra from the SMPS measurements and assuming a density of 1.4 g cm^{-3} (Larson et al., 1998; Park et al., 2003). The calculated concentrations C_{pp} were compared and verified with several Teflon-filter based mass measurements. The total hydrocarbon concentration in the CVS, C_{THC}, is calculated using the THC data (which are reported in units of ppmC) assuming a C/H ratio of 1.2. The fraction, F_{pp}, of the THC present in the primary particles in the exhaust in the CVS is calculated to be 0.21±0.07 using

$$F_{pp} = \frac{C_{pp}}{C_{pp} + C_{THC}} \quad (4)$$

F_{pp} did not change significantly over the narrow range of dilution ratios of 14–22 inside the CVS; however, it should decrease with dilution since C_{pp} is expected to decrease faster than C_{THC} due to evaporative loss of volatile organic components from the primary particles.

An aggregate partitioning coefficient K_p may be defined for the condensational uptake shown in Fig. 2 using

$$K_p = \frac{COM/M_s}{C_{THC}} = \frac{S}{C_{THC}} \quad (5)$$

or, $S = K_p C_{THC}$, and derived from the AMS measurements; C_{THC} is the concentration of THC in the flow tube. It should be noted that a true partitioning coefficient of a compound is determined only by its particle and gas phase concentrations, but in the absence of speciation information in both phases, the aggregate partitioning coefficient K_p as defined in Eq. (5) provides a convenient tool for modeling the organic mass that may reside in ambient particles from condensation of THC compounds in the engine exhaust. K_p may represent a pseudo Henry's law constant for the dissolving THC in the inorganic particles.

ACPD
11, 3461–3492, 2011

Figure 4 shows a plot of S versus C_{THC}, showing non-linear increases in S with increasing C_{THC}. A power function fitted to S versus C_{THC} yields

$$S = 0.012 + (1.37 \pm 0.28) \times 10^{-4} C_{THC}^{(2.53 \pm 0.76)} \quad (6)$$

with a correlation coefficient $r^2 = 0.81$ for the fit. S increases from 0.012 g/g to 0.26 g/g with C_{THC} increasing from 1 to 18 $\mu g\,m^{-3}$. The non-linearity shows that the partitioning coefficient K_p, being the derivative of the function given in Eq. (6), is not a constant with respect to C_{THC}. It increases from 0.0004 $(\mu g\,m^{-3})^{-1}$ at $C_{THC} = 1\,\mu g\,m^{-3}$, to 0.03 $(\mu g\,m^{-3})^{-1}$ at $C_{THC} = 18\,\mu g\,m^{-3}$, increasing by >100 times. The intercept (0.012) in the power function of Eq. (6) implies that at very high dilutions, the value of S becomes asymptotic. The relative size of this intercept may represent irreversible condensation (i.e. non-volatile compounds at STP) versus reversible equilibrium (SVOC, IVOC species).

The relationship between S and C_{THC} suggests that, as C_{THC} increases, proportionally more organics are partitioned into the particles, and the partitioning gradually moves to a regime where the saturation pressures may play an increasingly more important role in the partitioning compared to lower C_{THC}. Since the uptake was determined by the solubility of organics (see Figure 2b), the increasing S with C_{THC} may be due to enhanced solubility with the higher organic contents of the inorganic seed particles at the higher C_{THC}. Other factors not included in a simple solubility partitioning model, which can enhance the organic uptake and increase solubility under higher C_{THC}, include potential organic reactions in the particles (Liggio et al., 2007; Hallquist et al., 2009).

To compare with the partitioning between THC and the primary particle mass measured in the CVS, the fractions of THC condensed onto the seed particles are calculated as:

$$F_{com} = \frac{COM}{C_{THC}^0} = \frac{S \cdot M_s}{C_{THC}^0} \quad (7)$$

ACPD
11, 3461–3492, 2011

where C^0_{THC} is the initial THC concentration before dilution. Equation (7) shows that F_{com} varies linearly with respect to S if M_s and C^0_{THC} are fixed. For the experiments C^0_{THC} changed significantly while S varied over the dilution range of 81 to 2230 (Fig. 3). But there are no corresponding changes in the fraction F_{com} with the dilution ratio, suggesting that diluting both the gas and particle phase SVOCs did not cause systematic shifts in partitioning between the two phases.

For an M_s of 15 µg m^{-3} Eq. (7) yields an F_{com} between 0.02 and 0.21 and averages 0.12±0.06. For an M_s of 30 µg m^{-3}, F_{com} rises to a range between 0.07 to 0.4 and averages 0.21±0.09. Considering that F_{pp} is estimated at 0.21 for the low dilution situation inside the CVS and should decrease with further dilutions, F_{com} will be equivalent to F_{pp} at M_s lower than 30 µg m^{-3}. Thus, in moderately polluted atmosphere, the condensational uptake of SVOCs on inorganic particles can account for significant fractions of the THC emitted from gasoline engines, fractions that are equivalent to the primary particles.

3.5 Significance of condensational uptake: AURAMS regional air quality modeling

To test the significance of COM on a regional scale, a unified regional air quality modelling system, AURAMS (Gong et al., 2003; Stroud et al., 2008; Cho et al., 2009; Smyth et al., 2009; Slowik et al., 2010; also see Supporting Information, SI), was used to model the gasoline exhaust emissions and subsequent condensation of SVOCs onto $SO_4^=$ aerosol. Total gasoline exhaust organic vapor (THC) was treated as an additional gas-phase species in the mobile stream of the emissions processing system. THC was emitted, transported, lost by gas-phase chemistry, and allowed to reach equilibrium partitioning with $SO_4^=$ aerosol using Eq. (6). AURAMS was run at 15 km grid spacing with a domain covering eastern North America for the month of June, 2007. AURAMS produced concentration predictions for $PM_{2.5}$ $SO_4^=$, gasoline engine exhaust THC, total primary organic aerosol (POA) from all sectors, traditional

ACPD
11, 3461–3492, 2011

secondary organic aerosol (SOA), gasoline engine exhaust primary particulate mass and condensed organic mass (COM) from gasoline engine exhaust. The model was run over a high pollution episode (24 to 27 June) and a low pollution period (20 to 23 June).

During the high pollution episode, southerly flow brought air rich in $SO_4^=$ aerosol from the Ohio Valley to the Detroit-Windsor area; the maximum modeled $SO_4^=$ concentrations reached over 20 $\mu g\,m^{-3}$ on 26 June which is consistent with measured concentrations. The model captured some of the temporal behavior of the $SO_4^=$ data with a general small positive bias (Fig. S1, SI). In the Detroit-Windsor area, there were two noticeable maxima in the gasoline THC time series on 25 and 26 June. These days overlapped with the $SO_4^=$ event resulting in a large uptake of gasoline organic vapor to the $SO_4^=$ aerosol (maximum COM of 20 $\mu g\,m^{-3}$). The maximum COM from gasoline THC uptake was over an order of magnitude larger than the maximum gasoline engine primary organic aerosol maximum (gasoline exhaust POA, 0.7 $\mu g\,m^{-3}$) in the urban area.

Figure 5 shows the 3-day averaged model results over the high pollution episode from 24–27 June for a model domain centered over Lake Erie. While traditional SOA dominates the regional organic aerosol, in urban areas, COM was comparable to the total POA and was significant compared to urban SOA levels. For cleaner conditions, Figure 6 shows the 3-day averaged surface distributions for the period June 20 to 23. This was a period with northwesterly winds and low $SO_4^=$ over Windsor. Urban-scale gasoline exhaust COM to $SO_4^=$ in the Detroit-Windsor area air shed was less than the POA from all sectors and the modeled urban SOA. In the Detroit-Windsor area, the typical background gasoline COM was in the range 0.1 to 1 $\mu g\,m^{-3}$.

The model results show that by condensing onto sulfate particle alone, COM from SVOCs in the gasoline engine exhaust is already a significant amount in comparison with the total primary particle mass from all sources including gasoline exhaust. The amount of COM is higher than the total primary particle mass from all sources during the pollution episode across the model domain by a factor of up to 3, and higher than

ACPD
11, 3461–3492, 2011

the gasoline primary particle mass by up to a factor 7.5. One important feature is that COM is up to 50% of secondary organic aerosol mass in regions surrounding major urban centers. In the cleaner period, COM is still significant, being up to 75% of the total primary particle mass. In summary, the modeling results suggest that gasoline exhaust COM could be an important component of organic aerosol in urban areas with coincident high sulfate aerosol loadings.

It should be noted that the model application above uses $SO_4^=$ to derive the magnitude of COM over a regional scale. Other inorganic mass in the ambient particles may also serve as a good medium for the condensable organic materials to dissolve in, as shown in the experiments with NH_4NO_3 seed particle experiments. If these additional inorganic masses are included in the model application, COM will be larger than that based on $SO_4^=$ only, and relative to the primary particle mass the contributions from COM will be even higher over a regional scale. Furthermore, dissolution of SVOCs into the organic components in particles is probable and may further enhance COM.

4 Implications

The results presented above have implications for the emission databases used for modeling primary organic aerosol particles (POA), and for automotive emission control policies. The current emission data are based on results obtained under legislated methods for specific set of sampling conditions using filters at low dilution ratios (US EPA, 1993, 1996). No protocols are contained in the sampling guidelines to address the condensed organic mass on ambient particles. Thus, the primary particle mass emissions do not include the condensed organic mass as revealed in the present study. Consequently, current particle mass emissions underestimate the true POA emissions from automotive sources, neglecting an amount that can be similar to the primary particle mass.

ACPD
11, 3461–3492, 2011

Supplement related to this article is available online at: http://www.atmos-chem-phys-discuss.net/11/3461/2011/acpd-11-3461-2011-supplement.pdf.

Acknowledgements. Financial support for this research was from the PERD Particles and Related Emissions Program, Project C12.007.

References

Brook, R. D., Rajagopalan, S., Pope III, C. A., Brook, J. R., Bhatnagar, A., Diez-Roux, A. V., Holguin, F., Hong, Y., Luepker, R. V., Mittleman, M. A., Peters, A., Siscovick, D., Smith, S.C., Jr., Whitsel, L., and Kaufman, J. D.: Particulate matter air pollution and cardiovascular disease: an update to the scientific statement from the American Heart Association, Circulation, 121, 2331–2378, 2010.

Chase, R. E., Duszkiewicz, G. J., Richert, J. F. O., Lewis, D., Maricq, M. M., and Xu, N.: PM measurement artifact: Organic vapor deposition on different filter media, SAE, paper 2004-01-0967, 2004.

Cho, S., Makar, P. A., Lee, W. S., Herage, T., Liggio, J., Li, S. M., Wiens, B., and Graham, L.: Evaluation of a unified regional air-quality modeling system (AURAMS) using PrAIRie2005 field study data: The effects of emissions data accuracy on particle sulphate predictions, Atmos. Environ., 43, 1864–1877, 2009.

DeCarlo, P. F., Kimmel, J. R., Trimborn, A., Northway, M. J., Jayne, J. T., Aiken, A. C., Gonin, M., Fuhrer, K., Horvath, T., Docherty, K. S., Worsnop, D. R., and Jimenez, J. L.: Field-deployable, high-resolution, time-of-flight aerosol mass spectrometer, Anal. Chem., 78, 8281–8289, 2006.

Dockery, D. W., Pope, C. A., Xu, X., Spengler, J. D., Ware, J. H., Fay, M. E., Ferris, B. G. and Speizer, F. E.: An association between air pollution and mortality in six US cities, N. Engl. J. Med., 329, 1753–1759, 1993.

European Commission: Communication on the application and future development of Community legislation concerning vehicle emissions from light-duty vehicles and access to repair and maintenance information (Euro 5 and 6), available online at: http://eur-lex.europa.eu/LexUriServ/LexUriServ.do?uri=CELEX:52008XC0719(03):en:NOT, 2008.

ACPD
11, 3461–3492, 2011

Geller, M. D., Ntziachristos, L., Mamakos, A., Samaras, Z., Schmitz, D. A., Froines, J. R., and Sioutas, C.: Physicochemical and redox characteristics of particulate matter (PM) emitted from gasoline and diesel passenger cars, Atmos. Environ., 40, 6988–7004, 2006.
Gong, S. L., Barrie, L. A., Blanchet, J.-P., von Salzen, K., Lohmann, U., Lesins, G., and Spacek, L.: Canadian aerosol module: A size-segregated simulation of atmospheric aerosol processes for climate and air quality models 1. module development, J. Geophys. Res. 108, AAC 3-1 AAC 3-16, 2003.
Gong, W., Dastoor, A. P., Bouchet, V. S., Gong, S., Makar, P. A., Moran, M. D., Pabla, B., Ménard, S., Crevier, L.-P., Cousineau, S., and Venkatesh, S.: Cloud processing of gases and aerosols in a regional air quality model (AURAMS), Atmos. Res., 82, 248–275, 2006.
Grieshop, A. P., Miracolo, M. A., Donahue, N. M., and Robinson, A. L.: Constraining the volatility distribution and gas-particle partitioning of combustion aerosols using isothermal dilution and thermodenuder measurements, Environ. Sci. Tech., 43, 4750–4756, 2009.
Hallquist, M., Wenger, J. C., Baltensperger, U., Rudich, Y., Simpson, D., Claeys, M., Dommen, J., Donahue, N. M., George, C., Goldstein, A. H., Hamilton, J. F., Herrmann, H., Hoffmann, T., Iinuma, Y., Jang, M., Jenkin, M. E., Jimenez, J. L., Kiendler-Scharr, A., Maenhaut, W., McFiggans, G., Mentel, Th. F., Monod, A., Prévôt, A. S. H., Seinfeld, J. H., Surratt, J. D., Szmigielski, R., and Wildt, J.: The formation, properties and impact of secondary organic aerosol: current and emerging issues, Atmos. Chem. Phys., 9, 5155–5236, doi:10.5194/acp-9-5155-2009, 2009.
Jacob, D. J. and Winner, D. A.: Effect of climate change on air quality, Atmos. Environ., 43, 51–63, 2009.
Khalek, I. A., Kittelson, D., and Brear, F.: The influence of dilution conditions on diesel exhaust particle size distribution measurements, SAE, paper 1999-01-1142, 1999.
Kittelson, D. B.: Engines and nanoparticles: A review, J. Aerosol Sci., 29, 575–588, 1998.
Kwon, S.-B., Lee, K. W., Saito, K., Shinozaki, O., and Seto, T.: Size-dependent volatility of diesel nanoparticles: Chassis dynamometer experiments, Environ. Sci. Tech., 37, 1794–1802, 2003.
Larson, S. M., Cass, G. R., Hussey, K. J., and Luce, F.: Verification of image processing based visibility models, Environ. Sci. Tech., 22, 629–637, 1988.
Liggio, J., Li, S.-M., Brook, J., and Mihele, C.: Direct polymerization of isoprene and α-pinene on acidic aerosols, Geophys. Res. Lett., 34, L05814, doi:10.1029/2006GL028468, 2007.
Lipsky, E. M. and Robinson, A. L.: Effects of dilution on fine particle mass and partitioning of

ACPD
11, 3461–3492, 2011

semivolatile organics in diesel exhaust and wood smoke, Environ. Sci. Technol., 40, 155–162, 2006.
Liu, P. S. K., Deng, R., Smith, K. A., Williams, L. R., Jayne, J. T., Canagaratna, M. R., Moore, K., Onasch, T. B., Worsnop, D. R., and Deshler, T.: Transmission efficiency of an aerodynamic focusing lens system: comparison of model calculations and laboratory measurements for the Aerodyne Aerosol Mass Spectrometer, Aerosol Sci. Tech., 41, 721–733, doi:10.1080/02786820701422278, 2007.
Maricq, M., Chase, R., Podsiadlik, D., and Vogt, R.: Vehicle exhaust particle size distributions: a comparison of tailpipe and dilution tunnel measurements, SAE, paper 1999-01-1461, 1999.
Mathis, U., Ristimäki, J., Mohr, M., Keskinen, J., Ntziachristos, L., Samaras, Z., and Mikkanen, P.: Sampling conditions for the measurement of nucleation mode particles in the exhaust of a diesel vehicle, Aerosol Sci. Technol., 38, 1149–1160, 2004.
Mathis, U., Mohr, M., and Forss, A.-M.: Comprehensive particle characterization of modern gasoline and diesel passenger cars at low ambient temperatures, Atmos. Environ., 39, 107–117, 2005.
Onasch, T. B., Siefert, R. L., Brooks, S. D., Prenni, A. J., Murray, B., Wilson, M. A., and Tolbert, M. A.: Infrared spectroscopic study of the deliquescence and efflorescence of ammonium sulfate aerosol as a function of temperature, J. Geophys. Res., 104, 21317–21326, 1999.
Park, K. H., Cao, F., Kittelson, D. B., and McMurry, P. H.: Relationship between particle mass and mobility for diesel exhaust particles, Environ. Sci. Tech., 37, 577–583, 2003.
Pope III, C. A. and Dockery, D. W.: Health effects of fine particulate air pollution: lines that connect, J. Air Waste Manage. Assoc., 56, 709–742, 2006.
Prenni, A. J., DeMott, P. J., and Kreidenweis, S. M.: Water uptake of internally mixed particles containing ammonium sulfate and dicarboxylic acids, Atmos. Environ., 37, 4243–4251, 2003.
Robinson, A. L., Donahue, N. M., Shrivastava, M. K., Weitkamp, E. A., Sage, A. M., Grieshop, A. P., Lane, T. E., Pierce, J. R., and Pandis, S. P.: Rethinking organic aerosols: semivolatile emissions and photochemical aging, Science, 315, 1259, doi:10.1126/science.1133061, 2007.
Sakurai, J., Park K., McMurray, P. H., Zarling, D. D., Kittelson, D. B., and Ziemann, P. J.: Size-dependent mixing characteristics of volatile and nonvolatile components in diesel exhaust aerosols, Environ. Sci. Tech., 37, 5487–5495, 2003.
Schwarze, P. E., Orevik, J., Lag, M., Refsnes, M., Nafstad, P., Hetland, R. B., and Dybing,

ACPD
11, 3461–3492, 2011

E.: Particulate matter properties and health effects: Consistency of epidemiological and toxicological studies, Human Experiment. Toxicol., 25, 559–579, 2006.
Seinfeld, J. H. and Pandis, S. N.: Atmospheric Chemistry and Physics, John Wiley and Sons, New York, USA, 1998.
Shrivastava, M. K., Lipsky, E. M., Stanier, C. O., and Robinson, A. L.: Modeling semivolatile organic aerosol mass emissions from combustion systems, Environ. Sci. Tech., 40, 2671–2677, 2006.
Slowik, J. C., Stroud, C., Bottenheim, J. W., Brickell, P. C., Chang, R. Y.-W., Liggio, J., Makar, P. A., Martin, R. V., Moran, M. D., Shantz, N. C., Sjostedt, S. J., van Donkelaar, A., Vlasenko, A., Wiebe, H. A., Xia, A. G., Zhang, J., Leaitch, W. R., and Abbatt, J. P. D.: Characterization of a large biogenic secondary organic aerosol event from eastern Canadian forests, Atmos. Chem. Phys., 10, 2825–2845, doi:10.5194/acp-10-2825-2010, 2010.
Smyth, S. C., Jiang, W., Roth, H., Moran, M. D., Makar, P. A., Yang, F., Bouchet, V. S., and Landry, H.: A comparative performance evaluation of the AURAMS and CMAQ air-quality modelling systems, Atmos. Environ., 43(5), 1059–1070, 2009.
Stroud, C. A., Morneau, G., Makar, P. A., Moran, M. D., Gong, W., Pabla, B., and Zhang, J.: OH-reactivity of volatile organic compounds at urban and rural sites across Canada: Evaluation of air quality model predictions using speciated VOC measurements, Atmos. Environ., 42, 7746–7756, 2008.
US Environmental Protection Agency (US EPA): Emission factor documentation for AP-42, Technical Support Division, Office of Air Quality Planning and Standards, US Environmental Protection Agency, Research Triangle Park, NC, USA, 1993.
US Environmental Protection Agency (US EPA): Emission factor documentation for AP-42 Section 1.10 Residential Wood Stoves, US EPA, Washington DC, USA, 1996.

ACPD
11, 3461–3492, 2011

Table 1. Engine Operating Conditions and Gas and Primary Particle Characteristics in the Constant Volume Sampler (CVS).

Test Date	Engine Mode[a]	Primary Dilution Ratio	Average Gas Phase Concentrations in CVS			Primary Particle Mass and Number Size Distribution Characteristics in Primary Dilute Exhaust						
(2007)		$F_{cvs}/F_{exhaust}$	CO_2 (%)	NO_x (ppm)	THC (ppmC)	Total Mass ($\mu g\,m^{-3}$)[c]	Total Number (/cc)	Median (nm)	Mean (nm)	Mode (nm)	Geo. Mean (nm)	Geo. Std Dev
19 Apr	3	16.8	0.80	67.5	5.61	n/a	3.61E+7	9.0±1.7	9.2±1.7	8.8±1.9	9.0±1.6	1.1–1.4
20 Apr[b]	3	16.5	0.81	61.1	5.49	n/a	n/a	n/a	n/a	n/a	n/a	n/a
24 Apr	1	14.2	0.94	173	6.16	740±630	1.91E+8	13.6±3.6	14.1±3.6	14.2±4.6	13.2±3.2	1.3–1.5
	1	14.1	0.95	154	6.15	110±710	3.94E+8	12.6±2.0	12.9±2.0	13.2±2.6	12.2±1.8	1.2–1.5
25 Apr	2	22.3	0.60	68.3	6.68	220±140	2.09E+8	6.9±1.1	7.3±1.1	6.5±1.8	7.0±1.0	1.2–1.4
26 Apr	1	14.2	0.94	180	5.75	1350±370	4.81E+8	13.5±0.9	13.8±0.9	14.9±1.5	12.9±0.8	1.4–1.5
	1	14.2	0.94	180	6.22	2000±160	5.18E+8	15.0±0.9	15.3±0.8	16.5±1.2	14.2±0.7	1.4–1.5
27 Apr	3	16.8	0.80	57.6	6.09	850±400	4.65E+8	10.8±2.4	11.1±2.3	11.5±3.1	10.5±2.1	1.3-1.5
1 May	2	22.3	0.60	67.1	5.57	550±410	3.63E+8	10.1±2.4	10.5±2.3	10.5±3.1	9.9±2.0	1.3–1.5
	2	22.3	0.60	67.1	5.80	1260±210	4.93E+8	12.9±0.9	13.3±0.8	14.1±1.3	12.4±0.7	1.4–1.5
2 May	1	14.1	0.95	183	6.15	1930±170	4.55E+8	15.9±0.6	16.2±0.6	16.9±1.0	15.3±0.5	1.4–1.5
	1	14.2	0.94	182	6.14	2150±110	5.07E+8	15.9±0.6	16.1±0.6	17.0±1.1	15.2±0.5	1.4–1.5

[a] Mode 1: engine speed 1700 RPM, engine torque 73 ft-lb; Mode 2: engine speed 1700 RPM, engine torque 47 ft-lb; Mode 3: engine speed 2250 RPM, engine torque 47 ft-lb. [b] Particles in the primary dilute exhaust were not measured on 20 April 2007. [c] Total mass and number of the primary particles are derived from SMPS number size distributions after the SMPS reached steady-state, assuming a density of 1.4 $g\,cm^{-3}$ (Larson et al., 1988; Park et al., 2003). The SMPS did not reach a steady-state on 20 April.

ACPD
11, 3461–3492, 2011

Table 2. Uptake and condensation control parameter range during the study.

Date	Number of Experiments	Relative Humidity[a]	Exposure Time (min)	Seed Particle Size (nm)	Final Dilution Ratio
19 Apr	15	6.5–11.2		300	235–504
20 Apr	11	7.2–20.1		300	83
24 Apr	6	11.9–33.6		300	81
25 Apr	33	16.3–17.5	5.52	150, 200, 300, 350, 400	395
26 Apr	61	14.4–22.3	2.22–5.92	250, 300	140
27 Apr	45	16.5–28.7	5.53	300	96-672
1 May	74	16.7–22.4	5.53	250, 300, 350, 400	220
2 May	40	17.8–28	5.57	250, 300, 325, 450	127–2230
2 May	29	17.8–28	3.35–5.57	300	81–86

[a] When particles were exposed to gaseous exhaust.

ACPD
11, 3461–3492, 2011

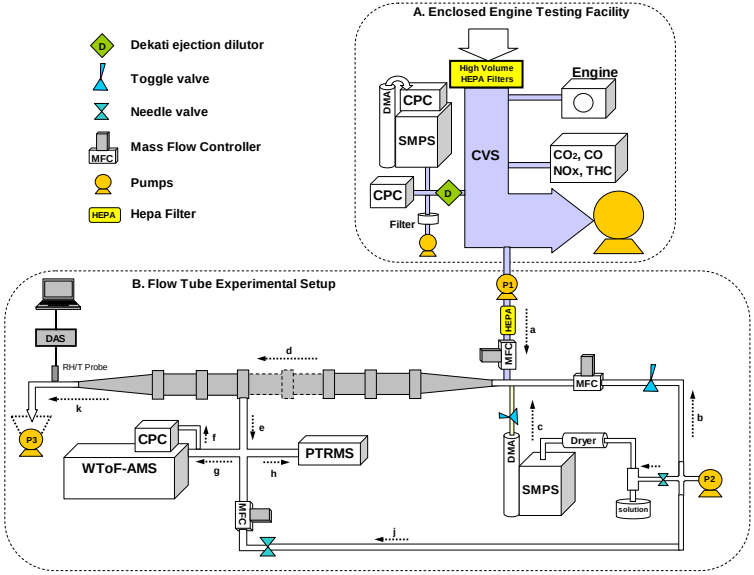

Fig. 1. An illustration of the experimental setup for this study. Section A shows the setup of the engine testing facility, where measurements of primary particles in the primary diluted exhaust in the CVS are made using SMPS, CPC, and filters. A small flow from the primary dilute exhaust in the CVS is pumped into the flow tubes, where it is mixed with laboratory generated seed particles. Arrows in Section B show the streams of air flow in the setup.

ACPD
11, 3461–3492, 2011

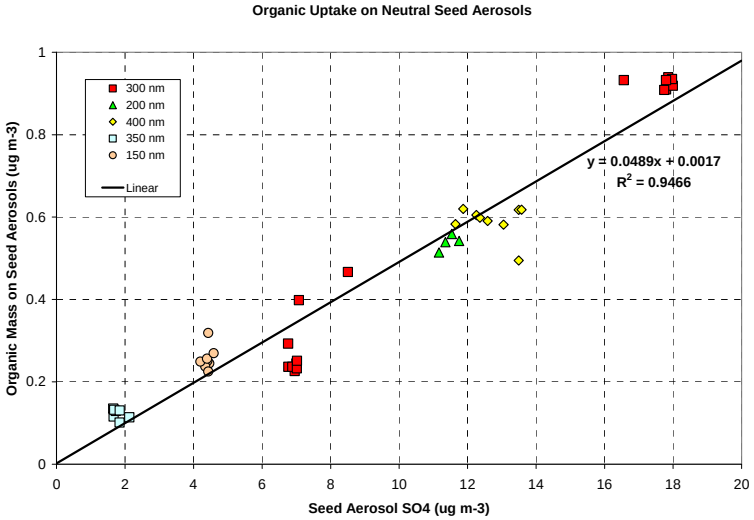

Fig. 2a. The condensed organic mass (COM) on sulfate seed particles. It is approximately a linear function of the available sulfate particle mass regardless of particle sizes.

ACPD
11, 3461–3492, 2011

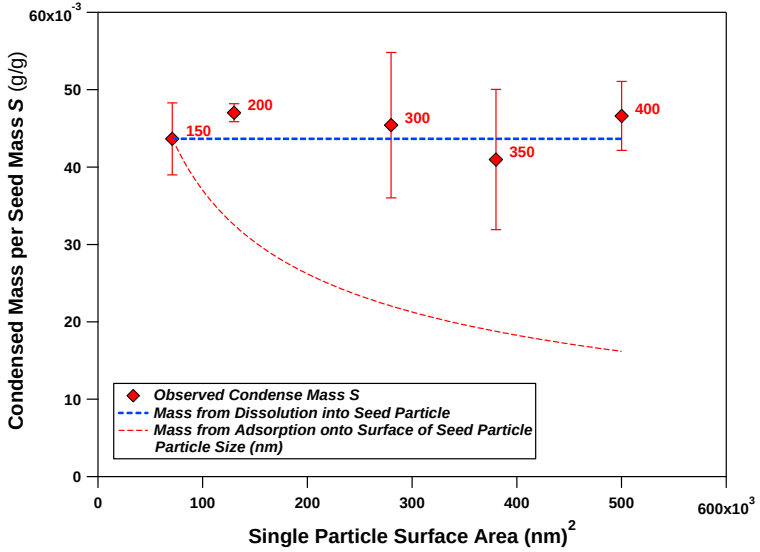

Fig. 2b. The COM/unit seed particle mass as observed, *S*, are derived as the slopes of organic mass versus seed particle mass for different particle sizes (e.g., Fig. 2a). Condensed mass from dissolution in the particle, relative to that at 150 nm seed particle, does not change with particle sizes (heavy dashed line); that from pure adsorption onto particle surface varies inversely with the surface area (light dashed line).

ACPD
11, 3461–3492, 2011

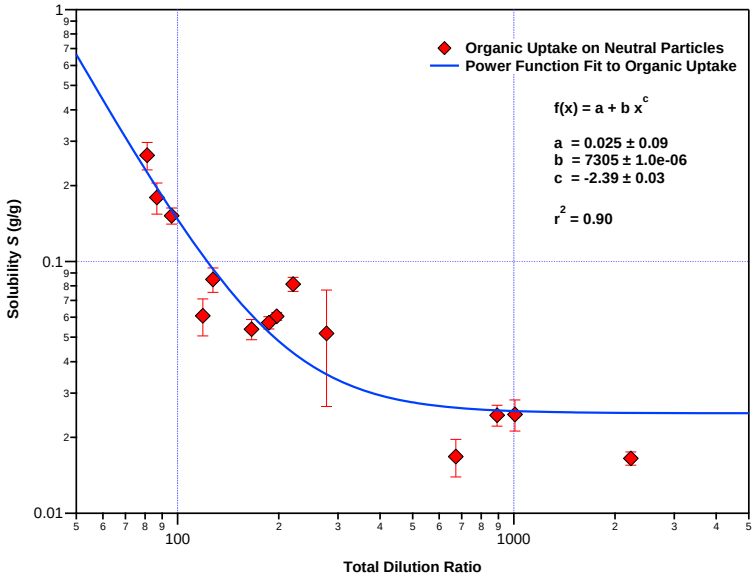

Fig. 3. The solubility *S* of the organic matter in the inorganic seed particles (condensed organic mass per unit mass of seed particles) versus total dilution ratios from 81 to 2230.

ACPD
11, 3461–3492, 2011

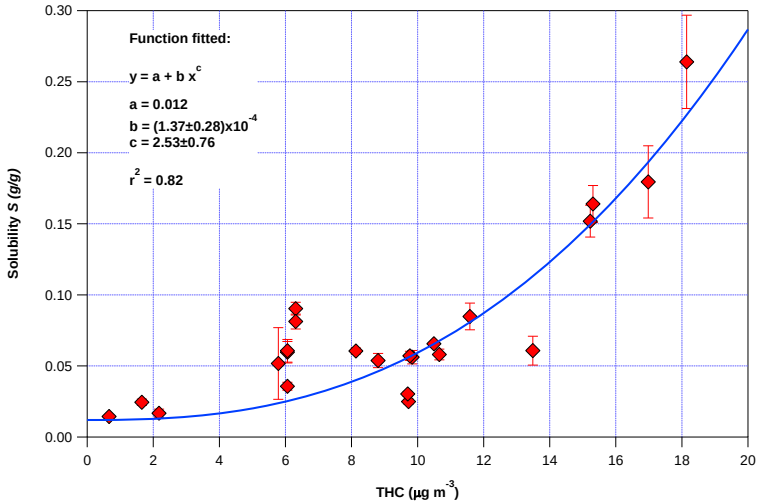

Fig. 4. The organic mass solubility in inorganic particles, S, versus the concentrations of THC in the gasoline engine exhaust, C_{THC}. A non-linear increase in S is observed with increasing C_{THC}. The relationship is fitted with a power function as shown by the fitted curve.

ACPD
11, 3461–3492, 2011

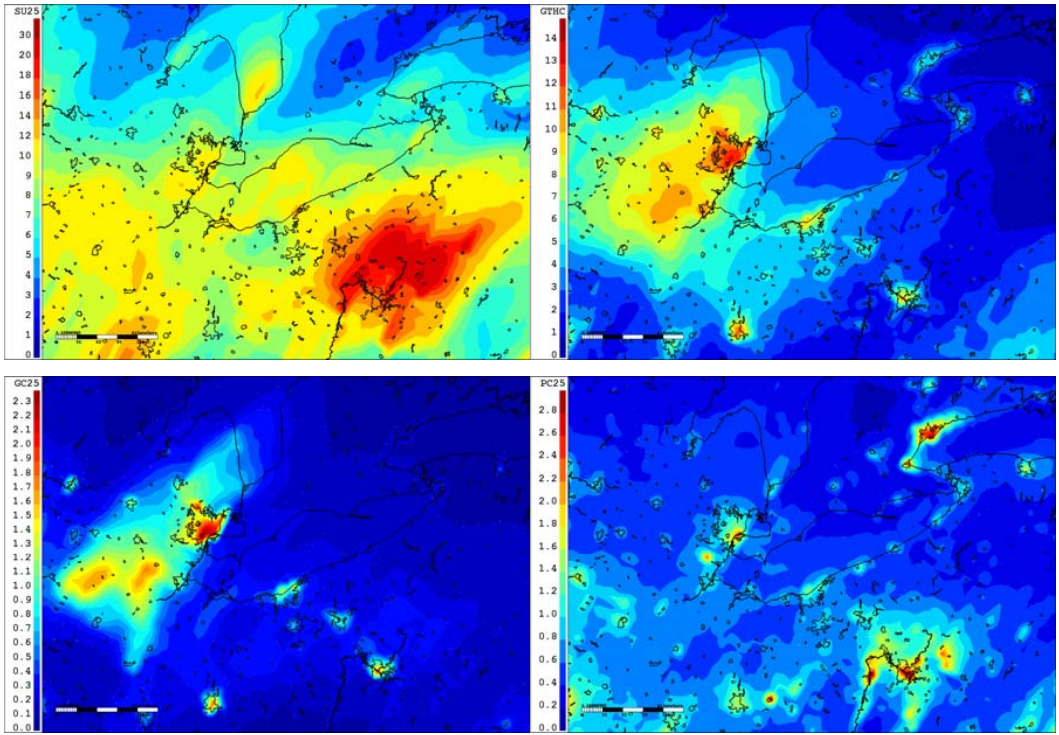

Fig. 5. Polluted Case, 24–27 June. Top left: Average surface $PM_{2.5}$ SO_4 ($\mu g\,m^{-3}$); top right: gasoline engine exhaust THC ($\mu g\,m^{-3}$), 2nd left: COM on SO_4 from the THC; 2nd right: $PM_{2.5}$ total primary particle mass from all sources ($\mu g\,m^{-3}$); 3rd left: $PM_{2.5}$ primary particle mass from gasoline exhaust only ($\mu g\,m^{-3}$); 3rd right: $PM_{2.5}$ SOA; bottom left: ratio of gasoline uptake to POA from all sectors; bottom right: ratio of gasoline uptake to POA from gasoline exhaust.

ACPD
11, 3461–3492, 2011

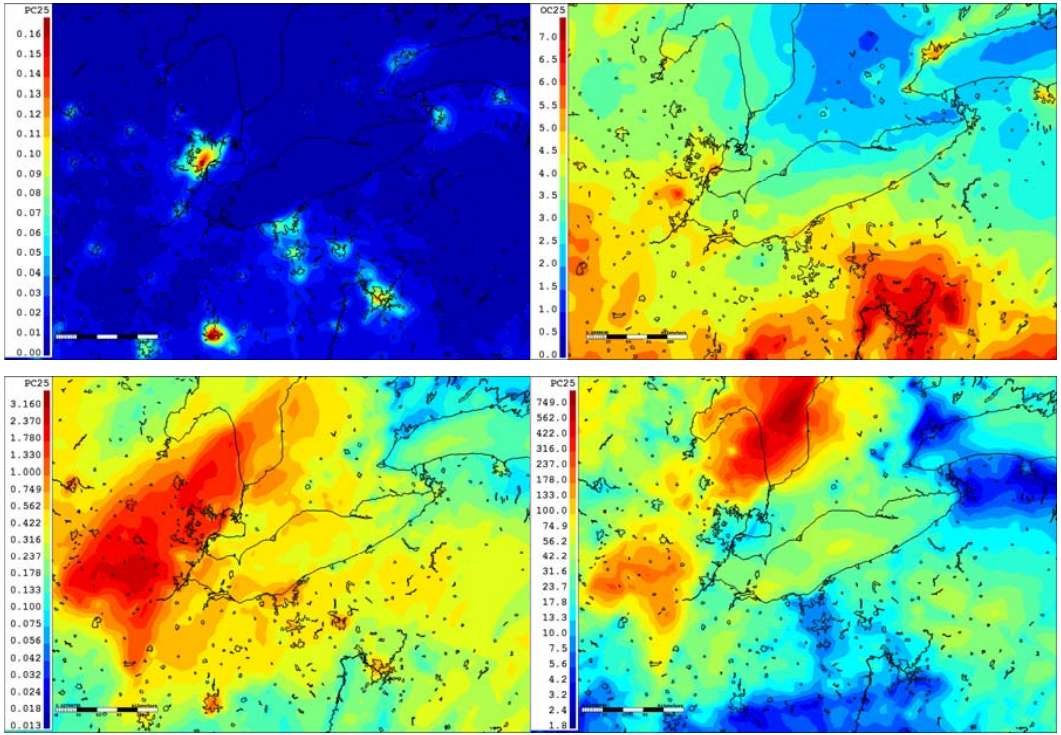

Fig. 5. Continued.

ACPD
11, 3461–3492, 2011

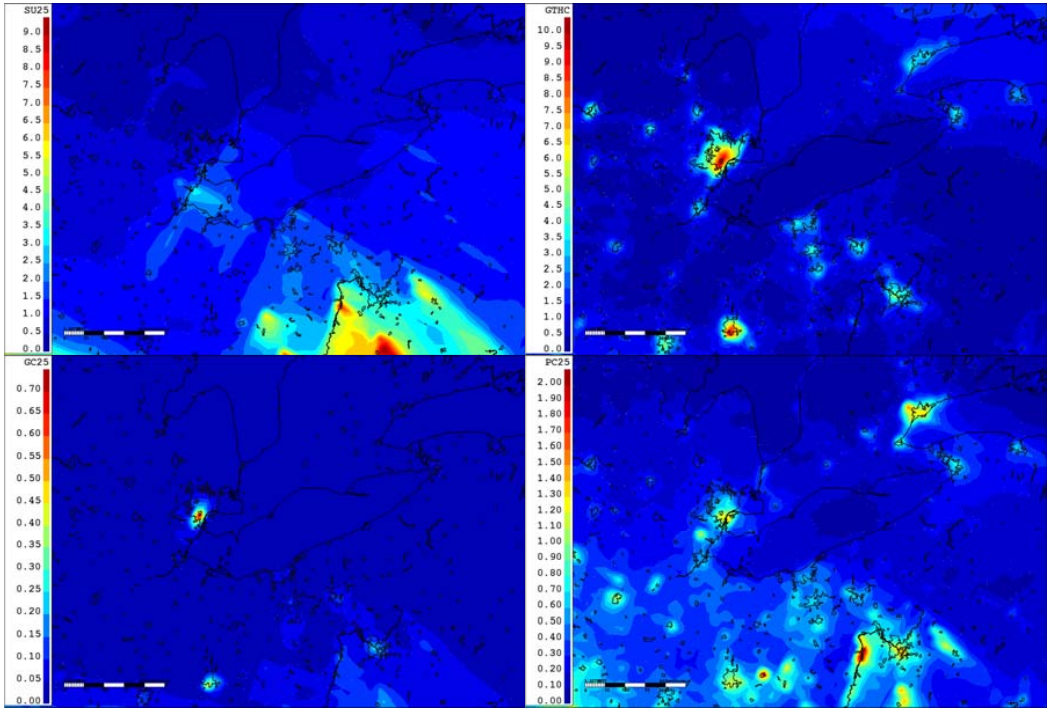

Fig. 6. Same as Fig. 5 but for Clean Case, 20 June 12:00 UTC.

ACPD
11, 3461–3492, 2011

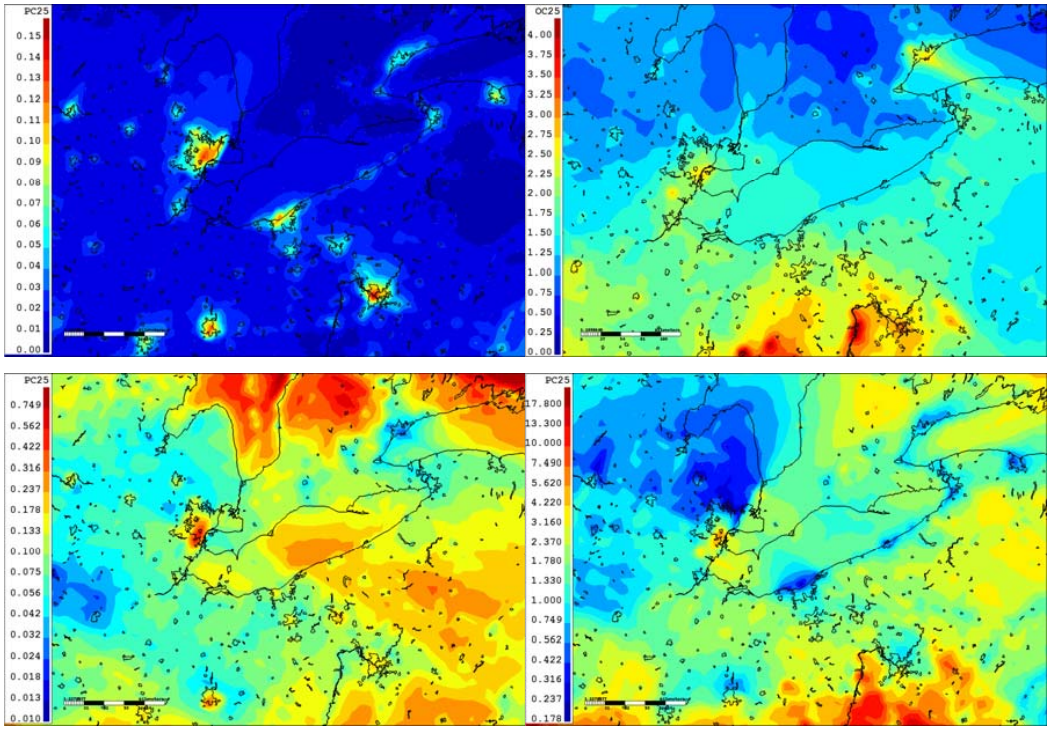

Fig. 6. Continued.

ACPD
11, 3461–3492, 2011